Journal of Organometallic Chemistry 839 (2017) 108–115

Contents lists available at ScienceDirect

Journal of Organometallic Chemistry

journal homepage: www.elsevier.com/locate/jorganchem

Ferrocenyl and cyrhetrenyl azines containing a 5-nitroheterocyclic moiety: Synthesis, structural characterization, electrochemistry and evaluation as anti-*Trypanosoma cruzi* agents

Johana Gómez [a], A. Hugo Klahn [a, *], Mauricio Fuentealba [a], Diego Sierra [b], Claudio Olea-Azar [c], Juan D. Maya [d], Manuela E. Medina [e]

[a] Instituto de Química, Pontificia Universidad Católica de Valparaíso, Casilla, 4059, Valparaíso, Chile
[b] Instituto de Química y Bioquímica, Universidad de Valparaíso, Av. Gran Bretaña, 1111, Valparaíso, Chile
[c] Departamento de Química Inorgánica y Analítica, Facultad de Ciencias Químicas y, Farmacéuticas, Universidad de Chile, Casilla 233, Santiago, Chile
[d] Programa de Farmacología Clínica y Molecular, Instituto de Ciencias Biomédicas, Facultad de Medicina, Universidad de Chile, Santiago, Chile
[e] Instituto de Ciencias de Materiales de Madrid, Consejo Superior de Investigaciones, Cientificas, Sor Juana Inés de la Cruz 3, 28049, Madrid, Spain

ARTICLE INFO

Article history:
Received 19 January 2017
Received in revised form
6 March 2017
Accepted 7 March 2017
Available online 11 March 2017

Keywords:
Cyrhetrenyl azines
Ferrocenyl azines
Structural characterization
Cyclic voltammetry
Trypanosoma cruzi
Chagas disease

ABSTRACT

The synthesis of unsymmetrical ferrocenyl and cyrhetrenyl azines [(η^5-C_5H_4)-CR=N-N=CH-2-C_4H_2X-5-NO_2]M (M=Re(CO)$_3$, Fe(η^5-C_5H_5); R = H, CH_3, X = O, S) has led to the development of new derivatives of 5-nitroheterocycles as potential anti-trypanosomal agents. The structures of compounds have been confirmed using conventional spectroscopic techniques (FT-IR, ^{1}H and ^{13}C NMR), mass spectrometry, including single-crystal X-ray diffraction analysis of compounds **2NT** and **4NT**. Based on the chemical shifts of the iminic carbons (C^6, C^7) and the reduction potential of the nitro group ($E_{1/2\ NO2}$), an extensive π-conjugation of the azine bridge (-C(R)=N-N=CH-) was observed along with a correlation between the opposing electronic effects of the cyrhetrenyl and ferrocenyl fragments. It was established that the existence of an electron-withdrawing group (cyrhetrene) could facilitate the generation of radical species (RNO_2 to $RNO_2^{\bullet-}$) through the azine bridge. The organometallic azines were evaluated for anti-trypanosomal activity *in vitro* against the epimastigote form of the Dm28c strain of *T. cruzi*, yielding IC_{50} values in the low micromolar range.

1. Introduction

Recognized by the World Health Organization (WHO) as one of the world's 13 most neglected tropical diseases (NTD), Chagas disease or American trypanosomiasis, is one of the most common endemic parasitic diseases in Central and South America, infecting 8–14 million people and causing significant deaths (14,000 per year) in this region [1,2]. The disease is caused by the protozoa *Trypanosoma cruzi (T. cruzi),* and current pharmacological treatments are limited to two nitroheterocyclic compounds, Nifurtimox (Nfx; Lampit®) and benznidazole (Bzn, Rochagan®), which contain a nitro group linked to a furan or imidazole ring, respectively [3,4]. These agents function as prodrugs and must undergo enzyme-mediated activation to have cytotoxic effects. These reactions are catalyzed by nitroreductases (NTRs) [5]. This chemotherapy, however, is usually unsatisfactory as the prodrugs showed poor clinical efficacy in the chronic phase of the disease and produced severe toxic side effects. Thus, Chagas disease remains a challenging infection due to the unavailability of safe, efficacious drugs [3,4,6].

The search for new antitrypanosomal agents has focused on several strategies. Various organic and inorganic compounds derived from nitro-heterocyclic systems have been extensively studied as anti *T. cruzi* agents. More recently, organometallic compounds have emerged as an auspicious alternative [7].

Metallocene-based chemotherapeutics are known to exhibit a wide diversity of biological activity [8]. Among them, ferrocenyl compounds have emerged as an important research field in the ongoing discovery of metallo-therapeutic agents (i.e., antibacterial, antitumor, antimalarial, and antitrypanosomal activities) [9–12].

Promising results have been reported for diseases such as cancer and malaria, indicating that the incorporation of a ferrocenyl fragment may enhance biological activities or generate new

* Corresponding author.
E-mail address: hugo.klahn@pucv.cl (A.H. Klahn).

http://dx.doi.org/10.1016/j.jorganchem.2017.03.014
0022-328X/

medicinal properties [13].

Additionally, the chemistry of cyrhetrene, [Re(η^5-C_5H_5)$(CO)_3$] (the typical example of a three-legged half-sandwich rhenium (I) complex), has undergone rapid development in the last decade [14]. Among its many other applications, this organometallic core has been recognized as a promising anticancer drug candidate [15]. For example, Re-Tamoxifen has been demonstrated to be slightly more active than Tamoxifen for the treatment of hormone-responsive breast tumors [16]. Recently, the cyrhetrenyl fragment was conjugated to sulfonamide moieties to target human carbonic anhydrases [17] and has also been incorporated into several pharmacophores for evaluation as potential antimalarial agents [18].

We have also reported the synthesis of several cyrhetrenyl and ferrocenyl-organic hybrids containing 5-nitrofuran and 5-nitrothiophene groups and evaluated their anti-*T. cruzi* activity. Although most reported compounds were less active than Nfx, we observed that antichagasic activity was dependent on the electronic nature of the organometallic groups and the π-conjugation of the bridge. Therefore, we established that these factors should be considered when designing new molecules with potential trypanocidal activity [11,12].

On the basis of this approach, we intend to develop new therapeutic agents for the treatment of Chagas disease by connecting ferrocenyl and cyrhetrenyl fragments (electron-donating or electron-withdrawing substituents, respectively) using a bioactive 5-nitroheterocycle ring. The results obtained from these studies have prompted us to expand our evaluation of organometallic fragments bound to 5-nitroheterocycle systems using an azine bridge. In this paper, we present the results of a detailed investigation on the synthesis and structural characterization (including X-ray) of unsymmetrical cyrhetrenyl and ferrocenyl-azines derived from 5-nitrothiophene (**1NT**-**4NT**). The results were compared to previously reported analogs containing 5-nitrofuran (**1NF**-**4NF**) [19]. Additionally, all compounds were evaluated for anti-trypanosomal activity against the Dm28c strain as a parasitic model and were found to have high antiparasitic effects *in vitro*. Due to its potential relevance in determining biological activity through generation of toxic free radicals via intra-parasite bioreduction, electrochemical behavior was investigated using cyclic voltammetry (CV). We also attempted to correlate the redox behavior of the ferrocene derivative compounds (**3NT**, **4NT**, **3NF**, **4NF**) to their propensity to oxidize.

The incorporation of azine, 2,3-diaza-1,3-butadiene bridge (commonly known as bis-Schiff bases) allowed us to evaluate electronic communication between the 5-nitroheterocycle ring and the organometallic groups to assess the relative influence of the electronic character of the organometallic fragments on the spectroscopic, structural and electrochemical properties, as well as the biological activity, of these molecules.

We considered these azine connectors because organometallic containing azines have gained recent attention due to their biological activities (i.e., as antimalarial and therapeutic agents), among their other remarkable applications in electrochemistry and coordination chemistry and as non-linear optical materials, molecular sensors, and catalyst precursors [10,20–22].

2. Results and discussion

2.1. Design and synthesis

The compounds were designed based on the backbone structure of Nifurtimox (Fig. 1a), a core structure with similar steric characteristics that allows different patterns of substitution on both sides of the azine bridge, i.e., the organometallic fragments and nitroheterocyclic groups that are both attached to the *C*-azine moiety. Moreover, the π-conjugation of the -C=N-N=C- system should allow electronic communication. In addition, our designed system allows varied substitution at the iminic carbon (R group) bound to the organometallic core (Fig. 1b). Structural diversity was also considered using bioisosterism between the 5-nitrofuran system and 5-nitrothiophene derivatives. That is, we varied the incorporation of oxygen and sulfur, since they have the same number of electrons in the valence shell but differ in several physical–chemical properties such as van der Waals radii, electronegativity, and lipophilicity. The ferrocenyl and cyrhetrenyl groups were chosen based on their opposite electronic effects (electron-donating or electron-withdrawing) (Fig. 1b).

The azine compounds derived from 5-nitrothiophene were prepared following the same procedure described for analogs of 5-nitrofuran [19]. This was accomplished via a condensation reaction between the corresponding substituted cyrhetrenyl hydrazine or ferrocenyl hydrazine [23,24] and 5-nitro-2-thiophenecarboxaldehyde, as indicated in Scheme 1. In all cases, the resulting compounds were isolated in low yield as pure material (by NMR) after purification by column chromatography and crystallization. All compounds were thermally stable, soluble in polar organic solvents and insoluble in hexane and benzene.

2.2. Characterization

The IR spectra of compounds **1NT** - **4NT** exhibited the expected absorption band for the ν(C=N) stretch in the range of 1606–1612 cm^{-1} in a CH_2Cl_2 solution and compared favorably to those measured for nitrofuran analogs [19]. However, this band shifted to lower wavenumber compared to that for a single organometallic imine derived from 5-nitrothiophene {[(η^5-C_5H_4)-N=CH(5-NO_2-2-C_4H_2S)]M, M=Re$(CO)_3$, Fe(η^5-C_5H_5) (1615-1637 cm^{-1})} [12]. This result can be interpreted as indicating efficient electronic delocalization between the metal fragment and the nitrothiophene ring through the azine bridge. Additionally, the shift of the asymmetric (ν_{as}) and symmetric (ν_s) stretching of the ν(CO) absorption bands of **1NT** and **2NT** to higher energies compared to those measured for the hydrazone precursors [Re{(η^5-C_5H_4)-C(R)=N-NH_2}$(CO)_3$] [23] further confirms that conjugation is increased by π-delocalization through the C=N-N=C moiety.

For all complexes, in addition to the hydrogen resonance characteristics of the cyrhetrenyl and ferrocenyl fragments, the ^{1}H NMR spectra of the nitrothiophene and azine portions of these molecules showed patterns similar to those previously reported for 5-nitrofuran analogs [19]. The ^{1}H NMR spectra indicated the presence of a single compound, as expected for these types of molecules. In addition, **2NT** and **3NT** exhibited singlets at approximately 2.28–2.41 ppm and 8.06–8.43 ppm, which were unequivocally assigned to the Me and –NC(H)- groups, respectively. The resonances of the two imine protons (H^6, H^7) in **1NT** and **2NT** are represented by singlets in the δ 8.14–8.56 range. In all cases, two doublets observed at approximately δ 7.25–7.91 were assigned to protons on the 5-nitrothiophene ring (H^9, H^{10}). The correct assignments of these resonances were carried out using 2D heteronuclear correlation NMR {^{1}H-^{13}C}-HMBC, {^{1}H-^{13}C}-HSQC and Dept-135.

As expected, ^{13}C{^{1}H} NMR data follow the same trend observed for the nitrofuran analogs [19]. That is, *i)* the iminyl carbon bound to the 5-nitrothiophene group is shielded from the organometallic iminyl carbon (C^6), *ii)* the deshielding of the C^7 in the cyrhetrenyl derivative compared with its ferrocenyl counterpart and *iii)* the low-field shift in the resonance of C^6 in the ferrocenyl analogs compared to the cyrhetrenyl analogs. These findings further confirm that the degree of electronic delocalization on the -C(R)=N-N=C(H)- unit is influenced by the electron-donating or electron-

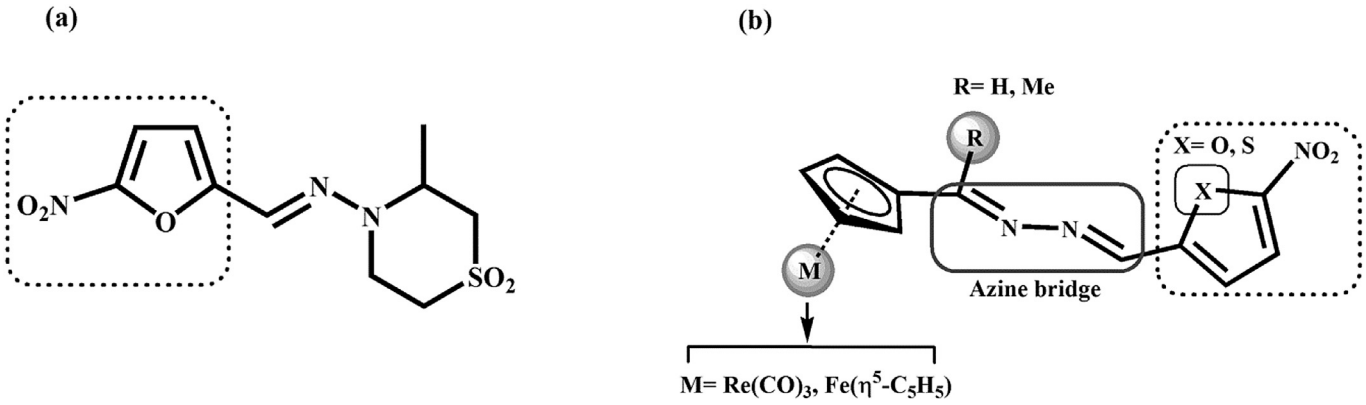

Fig. 1. (**a**) Nifurtimox (Nfx), (**b**) structural substitutions to the synthetic compounds.

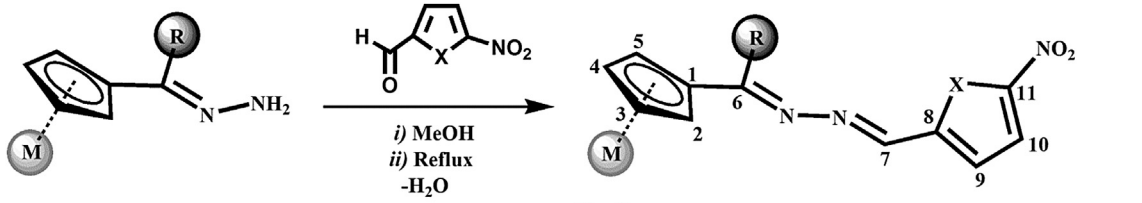

X = O

M = Re(CO)$_3$, R= H (**1NF**); M = Re(CO)$_3$, R= Me (**2NF**)
M = Fe(η^5-C$_5$H$_5$), R= H (**3NF**); M = Fe(η^5-C$_5$H$_5$), R= Me (**4NF**)

X = S

M = Re(CO)$_3$, R= H (**1NT**); M = Re(CO)$_3$, R= Me (**2NT**)
M = Fe(η^5-C$_5$H$_5$), R= H (**3NT**); M = Fe(η^5-C$_5$H$_5$), R= Me (**4NT**)

Scheme 1. - Synthesis of ferrocenyl or cyrhetrenyl azines derived from 5-nitrothiophene (**NT**) and 5-nitrofuran (**NF**) and the atom numbering system for NMR data.

withdrawing nature of the organometallic fragments.

Electron impact mass spectrometry was used to confirm the integrity of the synthesized compounds; in all cases the molecular ions were in agreement with the proposed structures.

2.3. X-ray structure analysis

To compare the structural parameters of 5-nitrothienyl azines with the crystallographic data reported for their analogs containing 5-nitrofuran and related compounds [19], single-crystal X-ray diffraction studies were successfully carried out for **2NT** and **4NT**. The bond lengths and bond angles are provided as supplementary materials (Tables S1 and S2). Views of the molecular structures with their atom numbering scheme (thermal ellipsoids with 50% probability) are shown in Fig. 2 for **4NT** and Fig. 3 for **2NT**.

In **2NT** (Fig. 3), the cyrhetrenyl group exhibited a typical three-legged piano stool structure, which is commonly observed for other half-sandwich rhenium (I) complexes [12,14e]. In **4NT** (Fig. 2), the ferrocenyl fragment adopted an eclipsed conformation, similar to that found in many other monosubstituted ferrocenyl derivatives [10,25].

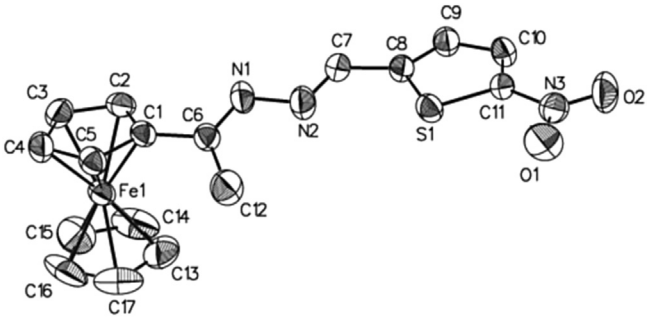

Fig. 2. - ORTEP drawing of the molecular structure of **4NT**. Selected bond lengths (Å): C1-C6, 1.485(12); C6-N1, 1.283(10); N1-N2, 1.427(10); N2-C7, 1.252(11); C7-C8, 1.463(12).

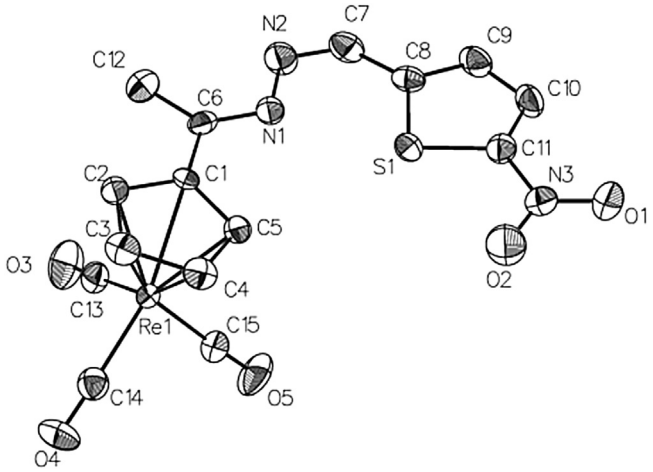

Fig. 3. - ORTEP drawing of the molecular structure of **2NT.** Selected bond lengths (Å): C1-C6, 1.461(7); C6-N1, 1.279(7); N1-N2, 1.406(5); N2-C7, 1.257(8); C7-C8, 1.436(7).

The **4NT** molecule exhibited a high degree of planarity along the $C_5H_4C(Me)NNC(H)C_4H_2S\text{-}5NO_2$ fragment (i.e., the dihedral angle between the $[C_5H_4C(Me)N1]$ and $[NC(H)C_4H_2S\text{-}5NO_2]$ least-square planes was only 1.8(3)°), whereas in compound **2NT**, the cyclopentadienyl ring and nitroheterocycle ring were less coplanar, forming a dihedral angle of approximately 12.7(17)° between the $[C_5H_4C(Me)N1]$ and $[NC(H)C_4H_2S\text{-}5NO_2]$ plane.

According to the X-ray diffraction data, azines may occur as three configurational isomers, namely, the (*E*,*E*), (*E*,*Z*) and (*Z*,*Z*) isomers [26]. The conformation of aromatic azines is controlled by a chain of four atoms: C=N-N=C and almost all studied aromatic azines exist in the preferred (*E*,*E*) configuration, in which the large groups attached to the C=N bonds are *trans* to the N–N bond [27,28]. In this regard, the **4NT** compound adopted an (*E*,*E*)-configuration for the -C(R)=N- moiety, and an *s-trans* conformation was observed around the N1-N2 bond, as reflected by the torsion angle of 175.1(3)°, as defined by the C6-N1-N2-C7 atoms. This stereochemistry is consistent with that previously reported for unsymmetrical cyrhetrenyl and ferrocenyl azines derived from 5-nitrofuran [19].

Nevertheless, compound **2NT** displays an (*E*,*Z*)-configuration, as the iminic bond C6-N1 displays (*E*)-isomerism. However, the N2-C7 bond exhibits an (*Z*)-configuration. This structural arrangement is not exceptional in the context of literature reports of the (*E*,*Z*) stereochemistry for some aromatic aldazines and ketazines [28,29]. It is important to note that the ketazine **2NT** adopts an *s-trans* conformation around the N1-N2 bond [torsion angle defined by the atoms C6-N1-N2-C7 of 177.6(5)°].

The sulfur atom was quite close to the H5 atom of the C_5H_4 unit. The H5···S1 [2.8303(12) Å] distance was clearly shorter than the sum of the van der Waals radii [S, 1.80 Å and H, 1.20 Å] of the two atoms. Hence, this hydrogen bond is an example of a "short" intramolecular contact [C5–H5···S1] (see supplementary materials, Fig. 1S) [30,31]. This intramolecular interaction may be induced by the electron-withdrawing character of "$Re(CO)_3$" fragment, decreasing the electron density in the cyclopentadienyl ring. This complex adopts (*E*,*Z*) stereochemistry to gain a more stable conformation.

The bond distances of the azine bridge in both structures are consistent with the N-N single bond and C=N double bond, which were previously reported for other organic and ferrocenyl azines [32,33]. For the 5-nitrothiophene group for **2NT** and **4NT**, the internal C-C, C-S and C-N(NO_2) bond distances were within the range found in organometallic Schiff bases derived from 5-nitrothiophene [12].

2.4. Electrochemical studies

To study the correlation between the electronic effects of the azine bridge substituents with their $E_{1/2\ NO2}$ and trypanocidal activity, we performed cyclic voltammetric experiments at room temperature. Fig. 4 shows, as an example, the cyclic voltammogram for **2NT** with a scan of 100–2000 mV^{-1}. All nitroheterocyclic complexes displayed comparable voltammetric behavior, showing two-defined reduction waves in a DMSO solution. As reported in previous studies [34,35], the first reduction wave for all compounds, which occurred in the potential range of −0.57 to −0.77 V, was correlated to a reversible process involving a one-electron transfer due to the reduction of Ar-NO_2 to a stable anion radical (i.e., Ar-NO_2^-). The reverse scan showed the anodic counterpart of the reduction wave. The subsequent more negative reduction wave (−1.07 to −1.37 V) belonging to the production of the hydroxylamine derivative (i.e., Ar-NHOH) [34] was irreversible for the entire range of sweep rates used (100-2000 mV^{-1}) for all compounds. Similar behavior was observed for organometallic Schiff bases

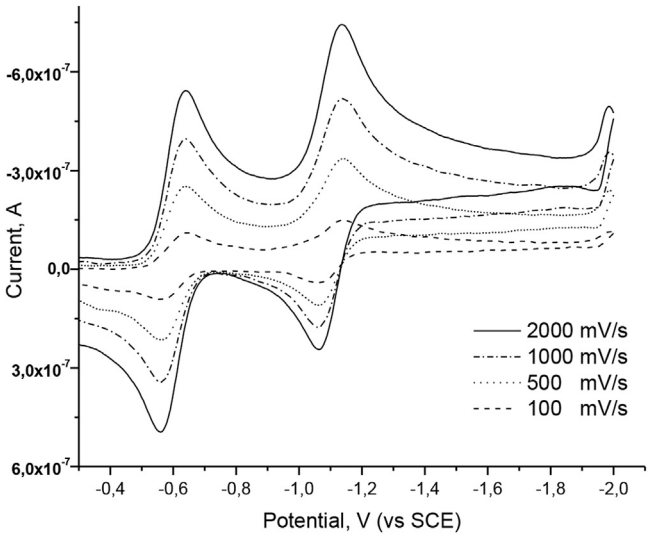

Fig. 4. - Cyclic voltammogram of **2NT** sweep rates from 100 to 2000 mV^{-1} in DMSO with 0.1 M TBAP.

derived from 5-nitrofuran and 5-nitrothiophene [12].

All azine derivatives exhibited lower $E_{1/2}$ ($E_{1/2} = (Ea + Ec)/2$) values than Nifurtimox, under the same conditions, with a greater capacity to be reduced than Nifurtimox ($E_{1/2\ NO2} = -0.88$ V, Table 1). Hence, these compounds had a better ability to generate radical species [35].

In the two series of compounds (**NT** and **NF**), the $E_{1/2\ NO2}$ values correlated with the electronic nature of the substituent attached to the azine bridge. The reduction potentials of Ar-NO_2 exhibited a cathodic shift for ferrocenyl azines ($E1/2$ NO2 = −0.66 to −0.71 V), due to the electron-donating ability of the ferrocenyl group. However, for the electron-withdrawing cyrhetrenyl fragment, anodic peak potentials were observed ($E1/2$ NO2 = −0.60 to −0.65 V, Table 1). These results confirm our previous observations concerning the close relationship between the electronic nature of the substituent and the ability of the nitro group to be reduced in these types of compounds, suggesting that electronic communication may exist between the two substituents of the azine core.

To correlate the oxidation potential of the ferrocenyl fragment with the reduction potential of the nitro group, the electrochemical properties of compounds **3NF, 4NF, 3NT, 4NT** were examined in CH_2Cl_2 solutions (1 mM) using 0.1 M [n-Bu_4N][PF_6] as the

Table 1
In vitro IC_{50}[a] values of azine compounds against *T. cruzi* epimastigotes (Dm28c strain) and their nitro group reduction potentials vs. a saturated calomel electrode in DMSO.

Compound	M	R	X	IC_{50} (μM) ± SE[b]	$E_{1/2\ NO2}$ (V)
1NF	Cy[c]	H	O	5.50 ± 1.65	−0.64
2NF	Cy	Me	O	5.73 ± 1.51	−0.65
3NF	Fc[d]	H	O	5.95 ± 1.61	−0.69
4NF	Fc	Me	O	9.69 ± 0.56	−0.71
1NT	Cy	H	S	8.90 ± 4.57	−0.60
2NT	Cy	Me	S	10.70 ± 1.59	−0.61
3NT	Fc	H	S	9.97 ± 1.30	−0.67
4NT	Fc	Me	S	18.20 ± 3.79	−0.66
Nfx[e]				10.20 ± 4.09	−0.88

[a] IC_{50}, concentration that inhibits 50% of growth. Values shown are the average of four or more experiments.
[b] Standard error (SE).
[c] Cy = (η^5-C_5H_4)$Re(CO)_3$.
[d] Fc = (η^5-C_5H_4)Fe(η^5-C_5H_5).
[e] Data from Ref. [35].

background electrolyte. A comparison of the relevant electrochemical data are given in Table 2. Ferrocenyl azines displayed similar voltammetric performance, and the observed redox behavior of the compounds was compared with that of ferrocene as a standard.

The separation of the voltammetric peaks (ΔEp ≈ 70 mV - 110 mV) and current ratios (*ipa*/*ipc*) was near unity, revealing that the ferrocene/ferrocenium couples [Fc/Fc^+] underwent an electrochemically reversible one-electron-step oxidation-reduction process [36].

Previous electrochemical studies on mono-substituted ferrocene derivatives have demonstrated that the presence of electron-donor groups increase the proclivity of the ferrocenyl unit to oxidation and the presence of electron withdrawing groups reduces the capacity of this fragment to be oxidized [36–38]. For all unsymmetrical ferrocenyl azines, the anodic peaks appeared at higher potentials than for ferrocene, indicating that these compounds became more difficult to oxidize (Table 2).

Consequently, a greater electron-withdrawing effect of the [C_5H_2X-NO_2] group over the azine bridge and the presence of the [-C(R)=N-] moiety in close proximity to the ferrocenyl fragment, should reduce electron density at the metal center, making the oxidation process more difficult (see supplementary materials, Fig. 2S) [38], suggesting that the azine bridge allows electronic communication between the 5-nitro-heterocycle and ferrocenyl fragment.

Finally, the shift toward a greater anodic potential of the ketazine (**4NF** and **4NT**) compared to the oxidation potential of the aldazines (**3NF** and **3NT**) suggest that the [-C(Me)=N-] entity has a greater electron-withdrawing effect than the [-C(H)=N-] moiety. Similar conclusions were found in electrochemical studies of ferrocenylimines {(η^5-C_5H_5)Fe(η^5-C_5H_4)–C(R^1)=N–R^2} [36].

2.5. In vitro anti-T. cruzi activity

To study the influence of the organometallic fragments incorporated into 5-nitroheterocyclic azines (**NF** and **NT**) on trypanocidal activities, the antiparasitic activity of all compounds was evaluated *in vitro* against the *T. cruzi* epimastigotes (Dm28c strain). Parasites were incubated with various concentrations of compounds to obtain a dose–response curve (cell viability (%) *vs* Log [M]) that allowed calculation of IC_{50} values (concentration that inhibits fifty percent of growth, with respect to an untreated control), including the Nifurtimox drug as a positive control. The results are shown in Table 1.

Most of the unsymmetrical ferrocenyl or cyrhetrenyl azines derivatives were active against epimastigotes of *T. cruzi*, Dm28c strain. Based on the IC_{50} values, the following trend was observed: *i)* the nitrofuran azines (**1NF** - **4NF**) were more active than the nitrothiophene analogs (**1NT** - **4NT**). This finding was in good agreement with other previously reported nitrofuran compounds with biological activity [39], *ii)* in both series of nitroheterocyclic compounds, the cyrhetrenyl derivatives were slightly better trypanocidal agents than their ferrocenyl counterparts, confirming our previous conclusion that the electron-withdrawing effects [12] and higher lipophilicity [18b] of this fragment are influencing factors on the biological activity, *iii)* aldazines showed increased parasitic activity compared to the corresponding ketazines; it is likely that the inductive effect of the Me group decreases the capability of the nitro group to be reduced (see electrochemical section), *iv)* the azine bridge increases trypanocidal activity when compared with similar compounds bridged by an imine moiety [12], indicating that π-conjugation facilitates electronic communication between organometallic and nitroheterocyclic groups; and *v)* we do not have a plausible explanation for the significant anti-trypanosomal activity found for the reported organometallic compounds. It could possibly be due to the presence of the ferrocenyl or cyrhetrenyl group that increases the cell permeability and lipophilicity of the compounds [18b,40]. We cannot rule out the hypothesis that better π-electron delocalization may also result in better inhibition activity in metal-containing compounds.

Table 2
- Redox potential of ferrocene and ferrocenyl azines derived from 5-nitroheterocycle.[a]

Compound	X	R	E_{pa} (V)	E_{pc} (V)	ΔE_p (mV)[b]	$E_{1/2}$ (V)[c]
Ferrocene	–	–	0.55	0.44	110	0.50
3NF	O	H	0.72	0.65	70	0.69
4NF	O	Me	0.74	0.67	70	0.71
3NT	S	H	0.74	0.66	83	0.70
4NT	S	Me	0.81	0.7	110	0.75

[a] Measured in CH_2Cl_2 at a scan rate of 100 mVs-1(V vs. Ag/AgCl(sat)).
[b] $\Delta Ep = E_{pc} - E_{pa}$.
[c] $E_{1/2} = (E_{pa} + E_{pc})/2$.

3. Conclusion

Unsymmetrical cyrhetrenyl and ferrocenyl azines containing the 5-nitrothiophene bioactive group were successfully synthesized and characterized using standard spectroscopic techniques and X-ray crystallography. A clear trend for the opposing electronic effects of the organometallic fragments was inferred from the chemical shifts (δ) of the azine bridge, -C(R)=N-N=C(H)-, as measured in the NMR spectra of all compounds.

We demonstrated that the electrochemical behavior of compounds (**1NF** - **4NF**, **1NT** - **4NT**), depends on the electronic properties of organometallic fragments connected through an azine bridge and a 5-nitroheterocycle ring. This phenomenon indicates that the introduction of an electron-donating group such as a ferrocenyl fragment (**3NF**, **4NF**, **3NT**, **4NT**) in the skeleton of the azine caused the complexes to exhibit more cathodic reduction potentials ($E1/2$ NO2 = −0.66 to −0.71 V) compared to those of their cyrhetrenyl analogs (**1NF**, **2NF**, **1NT**, **2NT**) ($E1/2$ NO2 = −0.60 to −0.65 V).

The synthesized compounds had potent *in vitro* activity (IC_{50} = 5.50–18.20 μM) against *T. cruzi* epimastigotes (Dm28c strain) of the same order of magnitude as that of Nifurtimox. These results indicated that the nitrofuran derivatives were more active than their nitrothiophene analogs. In all compounds, the replacement of a hydrogen atom with a methyl group on the imine organometallic carbon produced a decrease in trypanocidal activity. Upon increasing the conjugation of the bridge between the organometallic fragment and the heterocyclic ring, IC_{50} values considerably increased. Conjugation should therefore be considered an influencing factor for designing new compounds with potential antitrypanosomal activity.

4. Experimental

4.1. General remarks

The reactions were performed under a nitrogen atmosphere using standard Schlenk techniques. Solvents were obtained commercially, dried and distilled under nitrogen by standard methods prior to use. Ferrocene (98%), ferrocenecarboxaldehyde (98%), 5-nitro-2-thiophenecarboxaldehyde (98%), acetylferrocene (95%) and a *n*-Butyllithium solution (1.6 M in hexane) were obtained from Sigma-Aldrich. The complexes (η^5-C_5H_4COH)$Re(CO)_3$ [41] and (η^5-$C_5H_4COCH_3$)$Re(CO)_3$ [42] were prepared according to literature procedures. Silica gel 60 (Merck, particle size

0.063–0.200 mm) was used for TLC and column chromatography. Infrared spectra were recorded in a CH_2Cl_2 solution using a NaCl cell using a Perkin–Elmer model 1605 FT-IR spectrophotometer in the range 4000–800 cm^{-1}. ^1H and $^{13}C\{^1H\}$ NMR spectra and $\{^1H$-$^{13}C\}$-HMBC, $\{^1H$-$^{13}C\}$-HSQC and Dept-135 experiments were registered at 298 K using a Bruker AVANCE 400 III spectrometer (^1H NMR at 400.13 MHz and ^{13}C NMR 100.6 MHz) using $CDCl_3$ as a solvent and $SiMe_4$ as an internal reference. The chemical shifts are referenced to the residual deuterated solvent peaks. Chemical shifts (δ) are given in ppm, and the coupling constants (J) are given in Hz, [Abbreviations for the multiplicities of the signals detected in ^1H NMR: s (singlet), d (doublet), t (triplet) and br.s (broad singlet)]. Electron impact (EI) mass spectra were obtained using a Shimadzu GC-MS spectrometer (70 eV) at the Laboratorio de Servicios Analíticos, P. Universidad Católica de Valparaíso. Elemental analyses were measured on a Perkin-Elmer CHN Analyzer 2400.

4.2. Synthesis of cyrhetrenyl and ferrocenyl azines derived from 5-nitrothiophene. General procedure

The organometallic compounds derived from 5-nitrothiophene were synthesized following the same procedure as for 5-nitrofuran analogs [19]. Organometallic hydrazone [(η^5-C_5H_4)-C(R)=N-NH_2]M [M=$Re(CO)_3$, Fe(η^5-C_5H_5); R=H, CH_3] (1 eq.) and 5-nitro-2-thiophenecarboxaldehyde (2 eq.) were dissolved in anhydrous methanol (30 mL) with molecular sieves and refluxed for 6 h under a nitrogen atmosphere. The solvent was removed under vacuum. The residue was dissolved in CH_2Cl_2 and filtered through Celite, and the solution was evaporated under reduced pressure. Column chromatography on silica gel using hexane/CH_2Cl_2 (6:3) as the eluent moved a colored band that contained the product. The solid obtained after solvent evaporation was purified by crystallization from CH_2Cl_2/hexane (1:3) at −18 °C.

4.2.1. [Re{(η^5-C_5H_4)-C(R)=N-N=CH(5-NO_2-2-C_4H_2S)}$(CO)_3$] with R = H (**1NT**) or Me (**2NT**)

1NT: A dark yellow solid, Yield: 45%. IR (CH_2Cl_2, cm^{-1}): 2025 (s) (νCO), 1932 (vs) (νCO); 1612 (w) (νC=N). ^1H NMR ($CDCl_3$) δ: 5.45 (t, 2H, H^3 and H^4); 5.98 (t, 2H, H^2 and H^5); 7.31 (d, 1H, J = 4.2, H^9); 7.89 (d, 1H, J = 4.3, H^{10}); 8.33 (s, 1H, H^6); 8.56 (s, 1H, H^7). $^{13}C\{^1H\}$ NMR ($CDCl_3$) δ: 84.9 ($\underline{C}_5H_4$); 86.9 ($\underline{C}_5H_4$); 87,9 (C^1); 128.5 ($\underline{C}_4H_2S$); 130.1 ($\underline{C}_4H_2S$); 144.9 (C^8); 154.4 (C^7); 157.1 (C^6); 192.3 (Re-$\underline{C}O$). MS (based on ^{187}Re) m/z: 517 $[M]^+$; 589 $[M\text{-}CO]^+$; 461 $[M\text{-}2CO]^+$; 433 $[M\text{-}3CO]^+$. Anal. (%) Calc. for $C_{14}H_8N_3O_5SRe$: C, 32.56; H, 1.56 and N, 8.14; found: C, 32.52; H, 1.55 and N, 8.13. For **2NT**: A suitable clear yellow crystalline solid of this crop was used for X-ray crystal structure determination, yield: 46%. IR (CH_2Cl_2, cm^{-1}) 2028 (s) (νCO), 1936 (vs) (νCO); 1608 (w) (νC=N). ^1H NMR ($CDCl_3$) δ: 2.28 (s, 3H, $C\underline{H}_3$); 5.42 (t, 2H, H^3 and H^4); 6.00 (t, 2H, H^2 and H^5); 7.28 (d, 1H, J = 4.3, H^9); 7.88 (d, 1H, J = 4.2, H^{10}); 8.43 (s, 1H, H^7). $^{13}C\{^1H\}$ NMR ($CDCl_3$) δ: 15.2 ($\underline{C}H_3$); 85.1 ($\underline{C}_5H_4$); 86.8 ($\underline{C}_5H_4$); 127.5 ($\underline{C}_4H_2S$); 128.5 ($\underline{C}_4H_2S$); 147.4 (C^7); 156.5 (C^6); 192.6 (Re-$\underline{C}O$). MS (based on ^{187}Re) m/z: 531 $[M]^+$; 503 $[M\text{-}CO]^+$; 475 $[M\text{-}2CO]^+$; 447 $[M\text{-}3CO]^+$.

4.2.2. [(η^5-C_5H_5)Fe{(η^5-C_5H_4)-C(R)=N-N=CH(5-NO_2-2-C_4H_2S)}] with R = H (**3NT**) or Me (**4NT**)

3NT: Dark violet solid, Yield: 48%. **IR** (CH_2Cl_2, cm^{-1}): 1603 (w) (νC=N). ^1H NMR ($CDCl_3$) δ: 4.26 (s, 5H, $C_5\underline{H}_5$); 4.66 (t, 2H, H^3 and H^4); 4.91 (t, 2H, H^2 and H^5); 7.30 (d, 1H, J = 4.3, H^9); 7.91 (d, 1H, J = 4.2, H^{10}); 8.14 (s, 1H, H^7); 8.61 (s, 1H, H^6). $^{13}C\{^1H\}$ NMR ($CDCl_3$) δ: δ 69.9 ($\underline{C}_5H_5$); 70.2 ($\underline{C}_5H_4$); 72.7 ($\underline{C}_5H_4$); 76.2 (C^1); 127.5 ($\underline{C}_4H_2S$); 130.1 ($\underline{C}_4H_2S$); 137.7 (C^8); 148.5 (C^7); 156.1 (C^{11}); 165.8 (C^6). MS (m/z): 368 $[M]^+$. Anal. (%) Calc. for $C_{16}H_{13}N_3O_2SFe$: C, 52.33; H, 3.57 and N, 11.44; found: C, 52.22; H, 3.56 and N, 11.42. For **4NT**: A clear dark purple crystal was selected for X-ray crystallography, yield: 55%. IR (CH_2Cl_2, cm^{-1}): 1608 (w) (νC=N). ^1H NMR ($CDCl_3$) δ: 2.41 (s, 3H, $C\underline{H}_3$); 4.23 (t, 5H, $C_5\underline{H}_5$); 4.60 (t, 2H, J = 1.7, H^3 and H^4); 4.96 (t, 2H, J = 1.6 Hz, H^2 and H^5); 7.29 (d, 1H, J = 4.3, H^9); 7.91 (d, 1H, J = 4.4, H^{10}); 8.14 (s, 1H, H^7). $^{13}C\{^1H\}$ NMR ($CDCl_3$) δ: 16.1 ($\underline{C}H_3$); 69.2 ($\underline{C}_5H_4$); 69.9 ($\underline{C}_5H_5$); 71.9 ($\underline{C}_5H_4$); 80.6 (C^1); 127.6 ($\underline{C}_4H_2S$); 129.7 ($\underline{C}_4H_2S$); 137.6 (C^8); 145.6 (C^7); 156.1 (C^{11}); 171.4 (C^6). MS (m/z): 381 $[M]^+$.

4.3. Single-crystal X-ray diffraction studies

The **2NT** crystals were selected using a polarizing optical microscope and glued to a glass fiber for the single-crystal X-ray diffraction experiment. The X-ray intensity data were collected using a Bruker SMART CCD diffractometer equipped with normal focus, and the intensities were collected with graphite-monochromatized Cu-Kα radiation (λ = 1.54178). The data were collected over a hemisphere of reciprocal space using a combination of three sets of exposures. Each exposure of 30 s covered 0.3° in ϕ. The unit cell dimensions were determined by a least-squares fit of 60 reflections with I > 2 σ (I). The calculations were performed using SMART software [43] for data collection and data reduction.

The **4NT** crystal was mounted on MiTeGen MicroMounts™ in a random orientation. The diffraction data were collected at 296 K on a Bruker D8 QUEST diffractometer equipped with a bidimensional CMOS Photon100 detector using graphite-monochromated Mo-Kα radiation (λ = 0.71076). The diffraction frames were integrated using the APEX2 package [44] and corrected for absorption with SADABS [45]. In both cases, non-hydrogen atoms were refined using anisotropic displacement parameters, and H atoms were finally included in their calculated positions. The final R(on F) factor was 0.0265 for **2NT**, and 0.049 for **4NT**; wR(on $|F|^2$) = 0.0754 (**2NT**) [or 0.1101 (**4NT**)], and the goodness of fit = 1.170 and 1.070 (for **2NT** and **4NT**, respectively). Crystal data, data collection, the number of refined parameters, and further details concerning the resolution and refinement of the crystal structures of **2NT** and **4NT** are given in Table 3.

4.4. Electrochemical studies

Cyclic voltammetry studies were performed at room temperature using a Metrohm 693VA instrument equipped with a 694 VA Stand convertor and 693 VA Processor with a one-compartment three-electrode system containing a hanging mercury drop electrode (HMDE) as the working electrode, a platinum wire as the auxiliary electrode and a saturated calomel electrode (SCE) as the reference electrode. The reduction potentials of the complexes were measured using DMSO solutions, which were 4 mM in the sample and contained tetrabutylammonium perchlorate (TBAP, ca. 0.1 mol L^{-1}) as the supporting electrolyte in a three-electrode cell. All solutions were purged with nitrogen, and voltammograms were recorded under a blanket of nitrogen.

Cyclic voltammetric studies of the ferrocene/ferrocenium couple were performed at ambient temperature using a potentiostat ZRA SERIES G300 Electrochemical Analyzer with a one-compartment three-electrode system comprising a platinum disk working electrode, a platinum wire auxiliary electrode and an Ag/AgCl (sat) reference electrode. The reported $E_{1/2}$ values (see Table 2) refer to this electrode. Measurements were made using dichloromethane solutions, which were 1 mM in the sample and contained 0.1 M [n-Bu_4N][PF_6] as the background electrolyte. Unless otherwise stated, the scan rate used was 100 mV s-1. Under these conditions, the ferrocene/ferrocenium couple was used as a reference, with an $E_{1/2}$ of 0.50 V and ΔEp= 110 mV. All solutions were purged with argon, and voltammograms were recorded under a blanket of argon. The platinum working electrode was polished between runs.

Table 3
Summary of crystallographic data and details of the refinement of the crystal structures of compounds **2NT** and **4NT**.

	2NT	4NT
Empirical formula	$C_{15}H_{10}N_3O_5ReS$	$C_{17}H_{15}FeN_3O2S$
Formula weight	530.52	381.23
Temperature (°K)	296(2)	296.15
Crystal system	Triclínic	Monoclinic
Space group	P-1	$P2_1/n$
a/Å	7.3706(3)	5.8361(14)
b/Å	9.9499(4)	14.049(3)
c/Å	11.4101(4)	20.436(4)
α/°	90.124(2)	90.00
β/°	96.549(2)	95.327(8)
γ/°	95.768(2)	90.00
Volume ($Å^3$)	827.03(6)	1668.3(6)
Z	2	4
ρcalc (mg/mm^3)	2.130	1.518
Absorption coefficient (mm-1)	15.855	1.043
F(000)	504.0	784.0
Crystal size (mm^3)	0.2 × 0.2 × 0.1	0.221 × 0.128 × 0.062
2Θ range for data collection (°)	3.900–62.629°	4 to 52.94°
Index ranges	$-6 \le h \le 8, -11 \le k \le 8, -13 \le l \le 12$	$-7 \le h \le 7, -17 \le k \le 17, -25 \le l \le 25$
Reflections collected	3640	36819
Independent reflections	2565[R(int) = 0.0273]	3424 [R_{int} = 0.0989]
Data/restraints/parameters	2565/0/231	3424/0/218
Goodness-of-fit on F^2	1.170	1.070
Final R indexes[$I \ge 2\sigma$ (I)]	R_1 = 0.0265, wR2 = 0.0754	R_1 = 0.0490, wR2 = 0.1101
Final R indexes [all data]	R_1 = 0.0272, wR2 = 0.0759	R_1 = 0.0806, wR2 = 0.1240

4.5. Biological assays: in vitro antitrypanosomal activities

T. cruzi epimastigotes (Dm28c strain) were grown at 28 °C in Diamond's monophasic medium supplemented with 4 μM hemin and fetal calf serum, which was added to a final concentration of 5% (v/v). The compounds were prepared in 50 mM stock solutions in 100% DMSO, sonicated to enhance solubility and stored at −20 °C. Further dilutions were prepared on the day of the experiment. Nifurtimox was used as the reference drug in the experiment. The compounds were tested at a starting concentration of 100 μM–1 μM from a stock DMSO solution. The final DMSO concentration in the culture media never exceeded 0.2% (v/v) and had no effect by itself on the proliferation of parasites. The control was run in the presence of 0.2% DMSO and in the absence of any drug. Compounds dissolved in DMSO were added to suspensions of 3×10^6 epimastigotes/mL and incubated for 24 h at 37 °C. After this period, trypanocidal activity was measured using MTT assays as described elsewhere [46]. Briefly, MTT was added to a final concentration of 0.5 mg/mL with phenazine methosulfate (0.22 mg/mL) and incubated at 37 °C for 4 h. The parasites were solubilized in 10% sodium dodecyl sulfate-0.01 M HCl and incubated overnight. Formazan crystal formation was measured at 570 nm using an ELISA spectrophotometer (Labsystems Multiskan MS, Finlandia). A full dose-response curve was constructed for all compounds to determine the concentration inhibiting 50% of parasite growth (IC_{50} value). The IC_{50} values were obtained using non-linear dose-response curve-fitting analysis (log of concentration *vs* percentage of viable cells) via Graph Pad Prism 5 software [47]. Reported values are means of at least three independent experiments. Statistical significance was determined by Student's t-test to a confidence interval of 95%.

Acknowledgments

A.H.K. wishes to acknowledge FONDECYT-Chile (Projects 1150601 and 1110669), FONDEQUIP (Project EQM 130154) and D.I. Pontificia Universidad Católica de Valparaíso; J.G. wishes to acknowledge CONICYT and D.I. Pontificia Universidad Católica de Valparaíso for a postdoctoral position.

Appendix A. Supplementary data

Supplementary data related to this article can be found at http://dx.doi.org/10.1016/j.jorganchem.2017.03.014.

References

[1] M. Navarro, C. Gabbiani, L. Messori, D. Gambino, Drug Discov. Today 15 (2010) 1070–1078.
[2] D. Gambino, L. Otero, Inorg. Chim. Acta 393 (2012) 103–114.
[3] V. Delespaux, H.P. Koning, Drug. resist. Updat 10 (2007) 30–50.
[4] J.A. Urbina, Acta Trop. 115 (2010) 55–68.
[5] S.R. Wilkinson, J.M. Kelly, Expert. Rev. Mol. Med. 11 (2009) 1–24.
[6] L. Otero, P. Noblia, D. Gambino, H. Cerecetto, M. Gonzáles, J.A. Ellena, O.E. Piro, Inorg. Chim. Acta 344 (2003) 85–94.
[7] a) B. Muro, F. Reviriego, P. Navarro, C. Marín, I. Ramírez-Macías, M.J. Rosales, M. Sánchez-Moreno, V.J. Arán, Eur. J. Med. Chem. 74 (2014) 124–134;
b) P. Fricker, R.M. Mosi, B.R. Cameron, I. Baird, Y. Zhu, V. Anastassov, J. Cox, P.S. Doyle, E. Hansell, G. Lau, J. Langille, M. Olsen, L. Qin, R. Skerlj, R.S.Y. Wong, Z. Santucci, J.H. McKerrow, J. Inorg. Biochem. 102 (2008) 1839–1845;
c) M. Vieites, L. Otero, D. Santos, J. Toloza, R. Figueroa, E. Norambuena, C. Olea-Azar, G. Aguirre, H. Cerecetto, M. Gonzalez, A. Morello, J.D. Maya, B. Garat, D. Gambino, J. Inorg. Biochem. 102 (2008) 1033–1043.
[8] G. Erker, J. Organomet. Chem. 692 (2007) 1187–1197.
[9] a) M.R. Fouda, M.M. Abd-Elzaher, R.A. Abdelsamaia, A.A. Labib, Appl. Organometal. Chem. 21 (2007) 613–625;
b) U. Schatzschneider, N. Metzler-Nolte, Angew. Chem. Int. Ed. 45 (2006) 1504–1507;
c) C.G. Hartinger, N. Metzler-Nolte, P.J. Dyson, Organometallics 31 (2012) 5677–5685;
d) G. Gasser, N. Metzler-Nolte, Curr. Opin. Chem. Biol. 16 (2012) 84–91;
e) R.H. Fish, G. Jaouen, Organometallics 22 (2003) 2166–2177;
f) C.G. Hartinger, P.J. Dyson, Chem. Soc. Rev. 38 (2009) 391–401.
[10] W. Nkoana, D. Nyoni, P. Chellan, T. Stringera, D. Taylor, P.J. Smith, A.T. Hutton, G.S. Smith, J. Organomet. Chem. 752 (2014) 67–75.
[11] R. Arancibia, H. Klahn, G.E. Buono-Core, E. Gutierrez-Puebla, A. Monge, M.E. Medina, C. Olea-Azar, J.D. Maya, F. Godoy, J. Organomet. Chem. 696 (2011) 3238–3244.
[12] R. Arancibia, A.H. Klahn, G.E. Buono-Core, D. Contreras, G. Barriga, C. Olea-Azar, M. Lapier, J.D. Maya, A. Ibañez, M.T. Garland, J. Organomet. Chem. 743 (2013) 49–54.
[13] G. Jaouen, Bioorganometallics: Biomolecules, Labeling, Medicine, Wiley-Vch, 2006.
[14] a) Recent and relevant contributions on cyrhetrene derivatives A. Vessières, J. Organomet. Chem. 734 (2013) 3–16;
b) Y. Liu, B. Spingler, P. Schmutz, R. Alberto, J. Am. Chem. Soc. 130 (2008)

1554–1555;
c) G.A. Koutsantonis, P.L. Low, C.F.R. Mackenzie, B.W. Skelton, D.S. Yufit, Organometallics 33 (2014) 4911–4922;
d) T.S. Teets, J.A. Labinger, J.E. Bercaw, Organometallics 33 (2014) 4107–4117;
e) D. Sierra, N. Bhuvanesh, J.H. Reibenspies, J.A. Gladysz, A.H. Klahn, J. Organomet. Chem. 749 (2014) 416–420.
[15] A. Leonidova, G. Gasser, ACS. Chem. Biol. 9 (2014) 2180–2193.
[16] S. Top, A. Vessieres, P. Pigeon, M.N. Rager, M. Huche, E. Salomon, C. Cabestaing, J. Vaissermann, G. Jaouen, Chem. Bio. Chem. 5 (2004) 1104–1113.
[17] a) D. Can, B. Spingler, P. Schmutz, F. Mendes, P. Raposinho, C. Fernandes, F. Carta, A. Innocenti, I. Santos, C.T. Supuran, R. Alberto, Angew. Chem. Int. Ed. 51 (2012) 3354–3357;
b) C.T. Supuran, Nat. Rev. Drug Discov. 7 (2008) 168–181.
[18] a) L. Glans, W. Hu, C. Jöst, C. Kock, P.J. Smith, M. Haukka, H. Bruhn, U. Schatzschneider, E. Nordlander, Dalton Trans. 41 (2012) 6443–6450;
b) R. Arancibia, F. Dubar, B. Pradines, I. Forfar, D. Dive, A.H. Klahn, C. Biot, Bioorgan. Med. Chem. 18 (2010) 8085–8091;
c) R. Arancibia, C. Biot, G. Delaney, P. Roussel, A. Pascual, B. Pradines, A.H. Klahn, J. Organomet. Chem. 723 (2013) 143–148.
[19] J. Gómez, A.H. Klahn, M. Fuentealba, D. Sierra, C. Olea-Azar, M.E. Medina, Inorg. Chem. Commun. 61 (2015) 204–206.
[20] a) T. Stringer, H. Guzgay, J.M. Combrinck, M. Hopper, D.T. Hendricks, P.J. Smith, K.M. Land, T.J. Egan, G.S. Smith, J. Organomet. Chem. 788 (2015) 1–8;
b) V.A. Sauro, M.S. Workentin, Can. J. Chem. 80 (2002) 250–262;
c) S. Siangwata, N. Baartzes, Banothile C.E. Makhubela, Gregory S. Smith, J. Organomet. Chem. (2015) 26–32.
[21] C. López, R. Bosque, J. Arias, E. Evangelio, X. Solans, M. Font-Bardıa, J. Organomet. Chem. 672 (2003) 34–42.
[22] M. Emirik, K. Karaoglu, K. Serbest, U. Coruh, E.M. Vazquez-Lopez, Polyhedron 88 (2015) 182–189.
[23] J. Gomez, N. Leiva, R. Arancibia, J. Oyarzo, G.E. Buono-Core, A.H. Klahn, V. Artigas, M. Fuentealba, R. Bosque, G. Aullon, C. López, M. Font-Bardía, T. Calvet, J. Organomet. Chem. 819 (2016) 129–137.
[24] A.G. Osborne, M. Webba da Silva, M.B. Hursthouse, K.M.A. Malik, G. Opromolla, P. Zanello, J. Organomet. Chem. 516 (1996) 167–176.
[25] A. Houlton, N. Jasim, R. Roberts, J. Silver, D. Cunningham, P. McArdle, T. Higgins, J. Chem. Soc. Dalton Trans. (1992) 2235–2241.
[26] J. Safari, S. Gandomi-Ravandi, RSC Adv. 4 (2014) 46224–46249.
[27] J. Grzegorzek, Z. Mielke, A. Filarowski, J. Mol. Struct. 976 (2010) 371–376.
[28] R. Karmakar, C.R. Choudhury, S.R. Batten, S. Mitra, J. Mol. Struct. 826 (2007) 75–81.
[29] I. Alkorta, F. Blanco, J. Elguero, ARKIVOC VII (2008) 48–56.
[30] R. Taylor, O. Kennard, J. Am. Chem. Soc. 104 (1982) 5063–5070.
[31] G.R. Desiraju, T. Steiner, The weak hydrogen bond in structural chemistry and biology, in: IUCR Monographs on Crystallography vol. 9, Oxford University Press, Oxford, U.K., 1999.
[32] X. Xu-Bing, D. Chun-Ying, Z. Long-Gen, Y. Xiao-Zeng, Polyhedron 11 (1992) 1917–1922.
[33] F.H. Allen, O. Kennard, D.G. Watson, L. Brammer, A. Guy Orpen, J. Chem. Soc. Perkin Trans. II (1987) S1–S19.
[34] C. Olea-Azar, C. Rigol, F. Mendizabal, A. Morello, J.D. Maya, C. Moncada, E. Cabrera, R.D. Maio, M. Gonzales, H. Cerecetto, Free Rad. Res. 37 (2003) 993–1001.
[35] C. Olea-Azar, A.M. Atria, F. Mendizabal, R. di Maio, G. Seoane, H. Cerecetto, Spectrosc. Lett. 31 (1) (1998) 99–109.
[36] C. López, R. Bosque, S. Perez, A. Raig, E. Molins, X. Solans, M. Font-Bardia, J. Organomet. Chem. 691 (2006) 475–484.
[37] P.E. Kleyi, C.W. McCleland, T.I.A. Gerber, Polyhedron 29 (2010) 1095–1101.
[38] S.R. Gupta, P. Mourya, M.M. Singh, V.P. Singh, J. Organomet. Chem. 767 (2014) 136–143.
[39] M.M. Abd-Elzaher, A.A. Labib, H.A. Mousa, S.A. Moustafa, M.M. Abdallah, Res. Chem. Intermediat 40 (2014) 1923–1936.
[40] a) G. Jaouen, S. Top, A. Vessières, P. Pigeon, G. Leclercq, I. Laios, Chem. Commun. (2001) 383–384;
b) E.A. Hillard, A. Vessieres, S. Top, P. Pigeon, K. Kowalski, M. Huché, G. Jaouen, J. Organomet. Chem. 692 (2007) 1315–1326.
[41] J. Heldt, N. Fischer-Durand, M. Salmain, A. Vessières, G. Jaouen, J. Organomet. Chem. 689 (2004) 4775–4782.
[42] S. Jones, M. Rausch, P. Bitterwolf, J. Organomet. Chem. 396 (1990) 279–287.
[43] Bruker, SMART, Bruker AXS Inc.,, Madison, Wisconsin, USA, 2007.
[44] Bruker, APEX2, Bruker AXS Inc.,, Madison, Wisconsin, USA, 2007.
[45] Bruker, SADABS, Bruker AXS Inc.,, Madison, Wisconsin, USA, 2001.
[46] S. Muelas, M. Suárez, R. Pérez, H. Rodríguez, C. Ochoa, J. Escario, A. Gómez-Barrio, Mem. Inst. Oswaldo Cruz 97 (2002) 269.
[47] http://utsavbali.com/wp-content/uploads/2013/10/Prism5Regression.pdf.